ACTA UNIVERSITATIS AGRICULTURAE ET SILVICULTURAE MENDELIANAE BRUNENSIS

Volume LX 5 Number 5, 2012

# NOTCH ASPECTS OF RSP STEEL MICROSTRUCTURE

M. Černý, J. Filípek, P. Mazal, D. Varner

**Received: June 16, 2012**

## Abstract

ČERNÝ, M., FILÍPEK, J., MAZAL, P., VARNERD.: *Notch aspects of RSP steel microstructure.* Acta univ. agric. et silvic. Mendel. Brun., 2012, LX, No. 5, pp. 49–60

For a rather long time, basic research projects have been focused on examinations of mechanical properties for Rapid Solidification Powder (RSP) steels. These state-of-art steels are commonly known as "powdered steels". In fact, they combine distinctive attributes of conventional steel alloys with unusual resistance of construction material manufactured by so called "pseudo-powdered" metallurgy.
Choice of suitable materials for experimental verification was carried out based on characteristic application of so called "modern steel". First, groups of stainless and tool steel types (steel grades ČSN 17 and 19) were selected. These provided representative specimens for the actual comparison experiment. For stainless steel type, two steel types were chosen: hardenable X47Cr14 (ČSN 17 029) stainless steel and non-hardenable X2CrNiMo18-14-3 (ČSN 17 350) steel. They are suitable e.g. for surgical tools and replacements (respectively). For tooling materials, C80U (ČSN 19 152) carbon steel and American D2 highly-alloyed steel (ČSN "equivalent" being 19 572 steel) were chosen for the project. Finally, the M390 Böhler steel was chosen as representative of powdered (atomized) steels.
The goal of this paper is to discuss structural aspects of modern stainless and tool steel types and to compare them against the steel made by the RSP method. Based on the paper´s results, impact of powdered steel structural characteristics on the resistance to crack initiation shall be evaluated.

stainless steel, tool steel, powdered RSP steel, metallography, fracture behavior

Metallic materials have always played a significant role in history of mankind. Some metals (Au, Ag, Cu, Sn, Pb, Fe, and Hg) have been utilized for more than 2000 years. Iron processing ranked among the most important discoveries of the ancient world. Archeological period called "Iron Age" began in the Central Europe approximately in the seventh century BC (Ptáček, 2002). With gradual development of metallurgy, producers have reached limits in terms of material properties. This applies to cast, formed and thermally processed steels. Nevertheless the development has been going on even in this traditional area of metal processing industry. Curiously enough, in some procedures steel is not manufactured by die casting anymore. Some sort of "metal mass" is produced that is then turned into homogenous parts. Examples of such sophisticated mass include state-of-art powders with precise composition properties.

The powder is manufactured using physical-mechanical, chemical, electrochemical, and physical-chemical methods (Kraus 2011). Resulting powders are processed using hot or cold compaction. In this phase, pressurized conditions may be used. Then, sintering without or with the liquid phase is performed. Hot forming of these stocks and their thermal processing provide way of reaching unique properties that can never be achieved by the means of other technological procedures (Černý, 2012; Hosford *et al.*, 2007; Franta, 2012).

Manufacturing of machine parts made out of sintered steels began in the first half of the twentieth century. This production was economically favorable in case of parts with simple shaped and/or less stressed parts in mass production. Today powdered steels are extensively used e.g. for punches, metal splitting blades and other tools. All these parts must provide extreme durability and

fracture resistance. With standard steels, fracture strength is reduced structurally e.g. by notch effect of coarse carbide particles. These particles represent stress concentrators and are active during loading of the material. Minimal sizes and round shapes of carbides in powdered steels significantly increase values of critical fracture stress. Stress-developed pre-nucleation microcrack in the carbide fragmentation probably does not reach critical size for crack initiation resulting in grain destruction (Nauka o materiálu, 2012, Halbych, 2009). No wonder the RSP steels exhibit up to double strength values in comparison with standard steels. It is worth noting that RSP steels represent highly-desired combination of "conflicting" iron alloy properties: toughness and hardness.

## MATERIALS AND METHODS

Total of five steel samples were subject to metallographic analysis. They represent stainless and tool steel materials (Tab. I).

**Steel X2CrNiMo18-14-3** (ČSN 17 350) – chromium-nickel-molybdenum austenitic weldable steel with very low amount of carbon and resistant to intergranular corrosion. Suitable for food processing industry and medical science applications. This steel can be surgically inserted into bones. The sample was taken from a common hip joint implant.

**Steel X47Cr14** (ČSN 17 029) – chrome martensitic stainless steel. This steel is suitable for applications where hardness and wear-resistance are required. This includes kitchen knives, scissors, surgical instruments, gauges, and so on. The steel is not suitable for welding. The sample was taken from forged medical scalpel (both blade and handle).

**Steel C80U** (ČSN 19 152) – carbon-rich hardenable tool steel. Applications include forming/cutting tools and hand-operated tools.

**Steel X165CrMoV12** (D2, ČSN 19 572) – American steel with increased corrosion resistance. Applications include cutting tools, cold cutting tools, crushing tools and milling tools.

**M390 Böhler steel –** powdered steel that can be used to manufacture dies for plastics processing, pressure casting of metals/alloys and so on.

The samples were obtained by MTH® metallographic saw with of $Al_2O_3$ cutting disk (Halbich 2009, 2011). To observe and display the structure of the material, the following equipment was used: Neophot 32 light microscope for low-zoom images; SEM (Scanning Electron Microscope) for high-zoom imaging and spectral analysis.

## RESULTS

**Austenitic Steel X2CrNiMo18-14-3** (ČSN 17 350)

Fig. 1 shows steel structure with uniform dispersion of fine carbide grains. Mosaic pattern of carbides on the edges of austenitic grains is clearly visible. Carbides do not create conditions (carbide clusters) to form typical defects of this steel type due to dispersion refinement and steel purity. Dissolution of carbides can be achieved by annealing at 1100 °C and water cooling, which produces homogeneous austenite with high corrosion resistance.

In the supplied state (annealed), structure of this steel is formed by pearlite with coarser globular carbide grains. Low-carbon martensite, residual austenite and carbides appear in the structure after thermal processing.

Hardening procedure and its reason are obvious when we compare typical snapshots of blade and shank structure. Snapshots of the blade (see Fig. 2) show martensite (with structural inclusions) in prevailing plate habitus that contains uniformly dispersed fine chromium carbides. They are located particularly on the grain edges. The location may result in severe chipping (!). The shank is annealed primarily. Martensite is acicular. Inclusions and homogeneously distributed structural carbides are situated on the edge of martensitic needles. Tempering above 300 °C supports evolution of very fine carbides.

**Steel C80U** (ČSN 19 152)

Fig. 3a shows granular pearlite with sulfide inclusions that form distinct row forming.

I: *Stainless and tool steel types*

| Steel Type | | | C | Mn | Si | Cr | Ni | Mo | W | V |
|---|---|---|---|---|---|---|---|---|---|---|
| EN | ČSN | Trade name | % | | | | | | | |
| X2CrNiMo18-14-3 | 17 350 | | max 0,03 | max 2,0 | max 1,0 | 16,5<br>18,5 | 12,0<br>15,0 | 2,50<br>3,00 | | |
| X47Cr14 | 17 029 | | 0,40<br>0,50 | max 0,90 | max 0,70 | 14,0<br>16,0 | | | | |
| C80U | 19 152 | | 0,75<br>0,90 | 0,20<br>0,40 | 0,15<br>0,35 | max 0,2 | max 0,25 | | | |
| X165CrMoV12 | 19 572 | D2<br>(AISI) | 1,45<br>1,70 | 0,20<br>0,45 | 0,20<br>0,42 | 11,0<br>12,5 | | 0,40<br>0,60 | | 0,15<br>0,30 |
| | | M390<br>(Böhler) | 1,9 | 0,3 | 0,7 | 20 | | 1 | 0,6 | 4 |

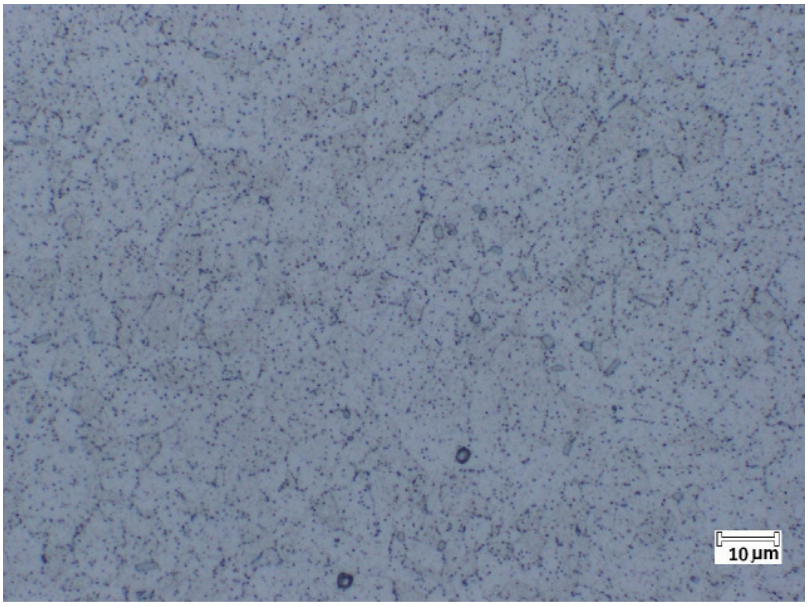


1: *Steel X2CrNiMo18-14-3 (ČSN 17 350)*

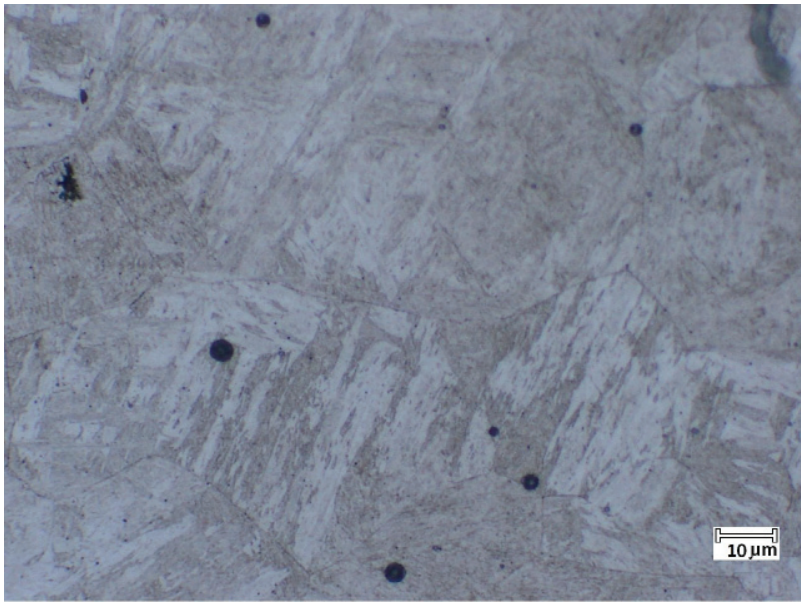


2: *Steel X47Cr14 (ČSN 17 029)*

The material can be annealed to allow for easy machinability. Its default structural dispersion is suitable for hardening. From the energetic point of view, this state provides a good initial state for development of fine-grained martensitic structure with suitable carbides dispersion (see Fig. 3b). Tempering of martensite (see Fig. 3c) does not radically alter the structure. In terms of stress condition, residual stress (the second kind) decreases. This behavior is then reflected by decrease in hardness and increase in toughness as well.

**D2 Steel**

Highly-alloyed American steel is delivered in annealed state. It features specific structure of pearlite (see Fig. 4a). Typical ferrite patterns more emphasized than with ČSN 19 152 steel. Grains are mostly uniform in size, what makes the material feasible for subsequent austentization. Thanks to alloy components, hardening and tempering at secondary hardness produces excellent alloy properties. After tempering, ledeburitic phase with secondary carbides seems to be the most important structural element (see Fig. 4b). The appearance of alloy with secondary carbides is not affected by rise of quench-hardening temperature. The longer

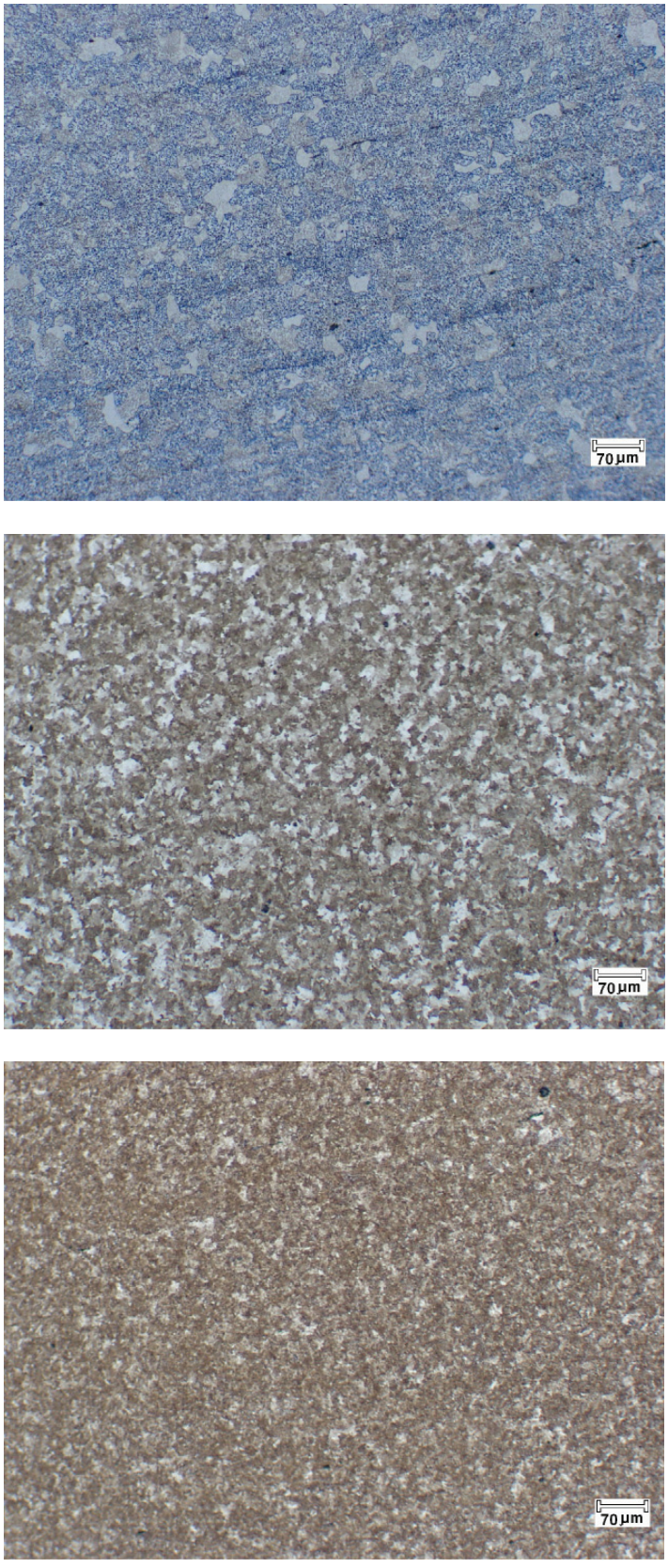


3: *C80U Steel (ČSN 19 152)*
a – No heat treatment
b – Hardened at 900 °C
c – Hardened at 900 °C and tempered

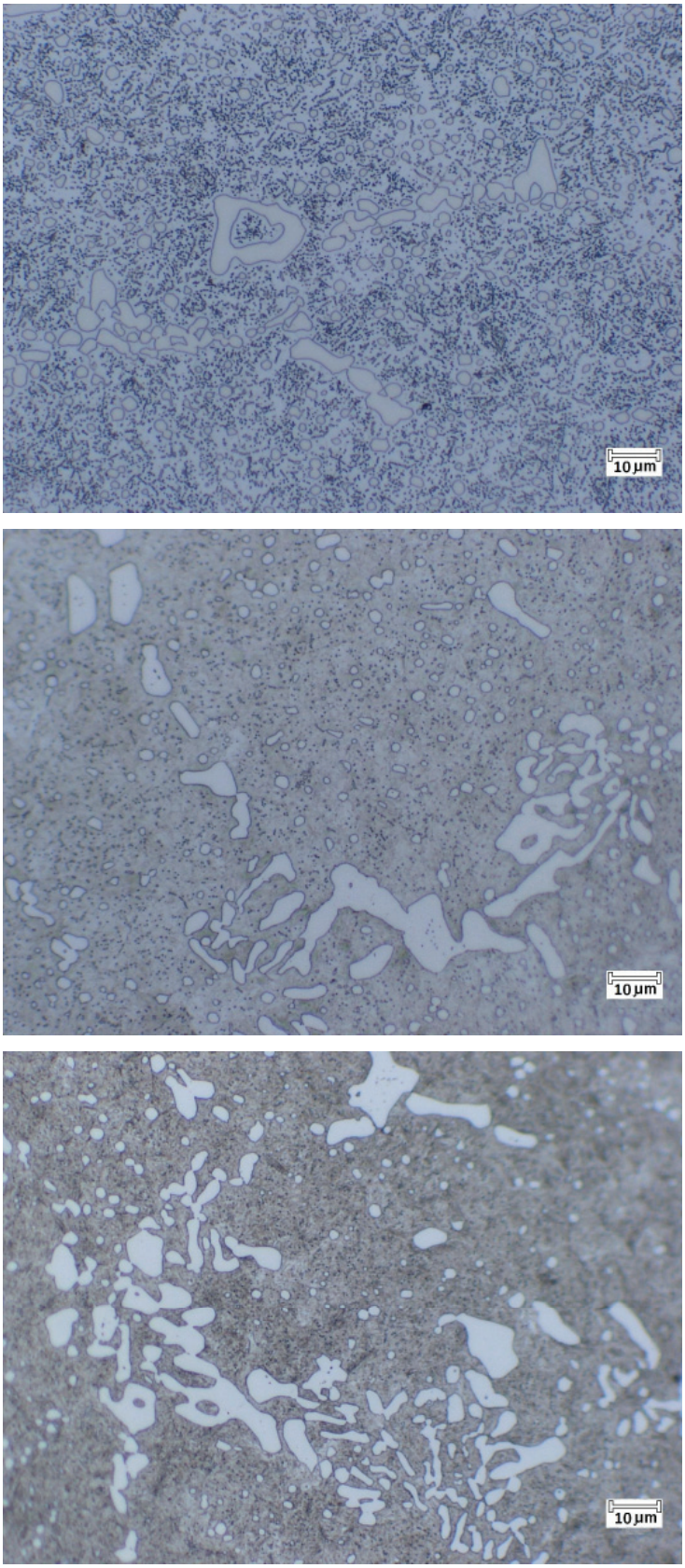


4: *D2 Steel*
a – No heat treatment
b – Hardened at 1 050 °C for 10 minutes
c – Hardened at 1 050 °C for 30 minutes and tempered

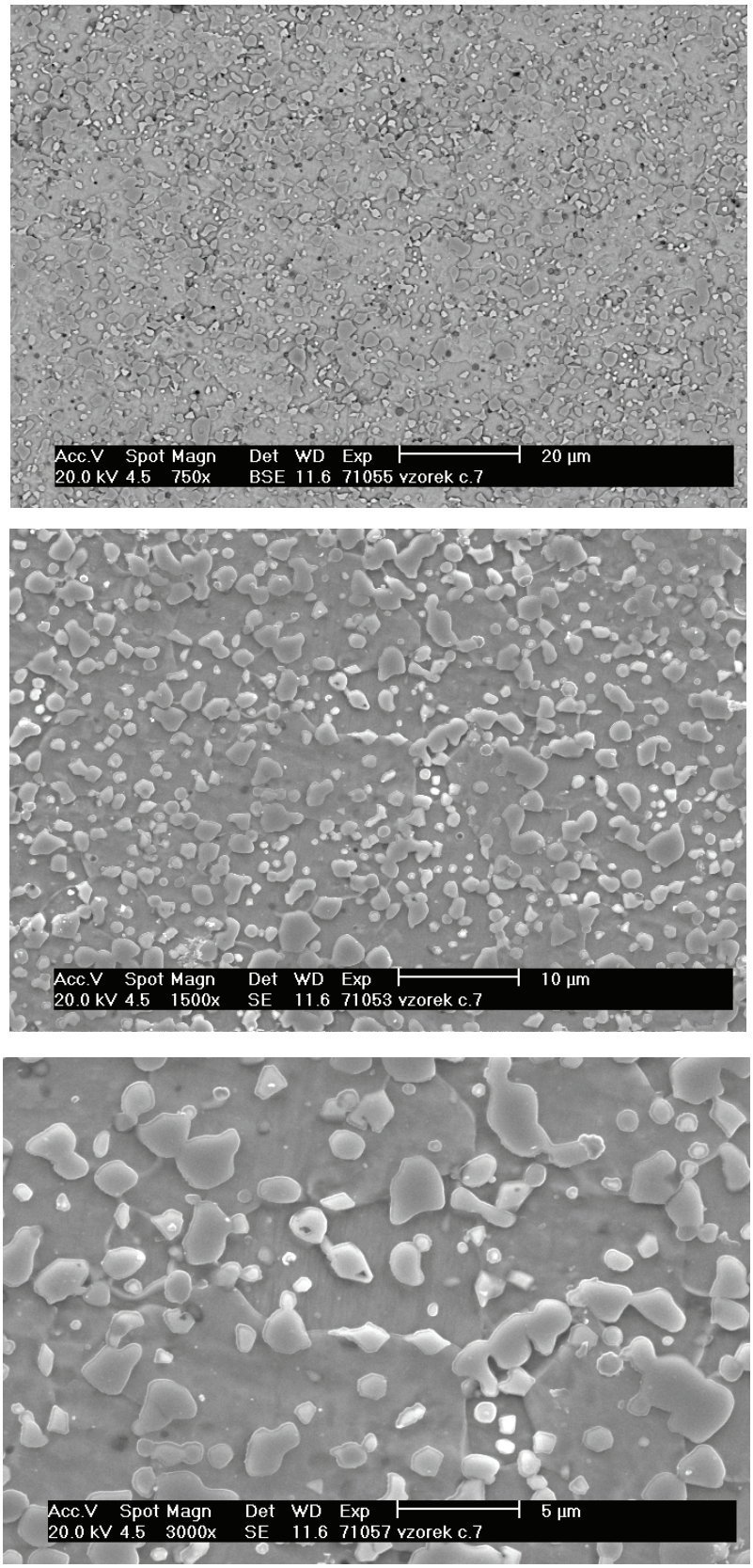


5: *M 390 Böhler steel, original state*
a – 750×
b – 1 500×
c – 3 000×

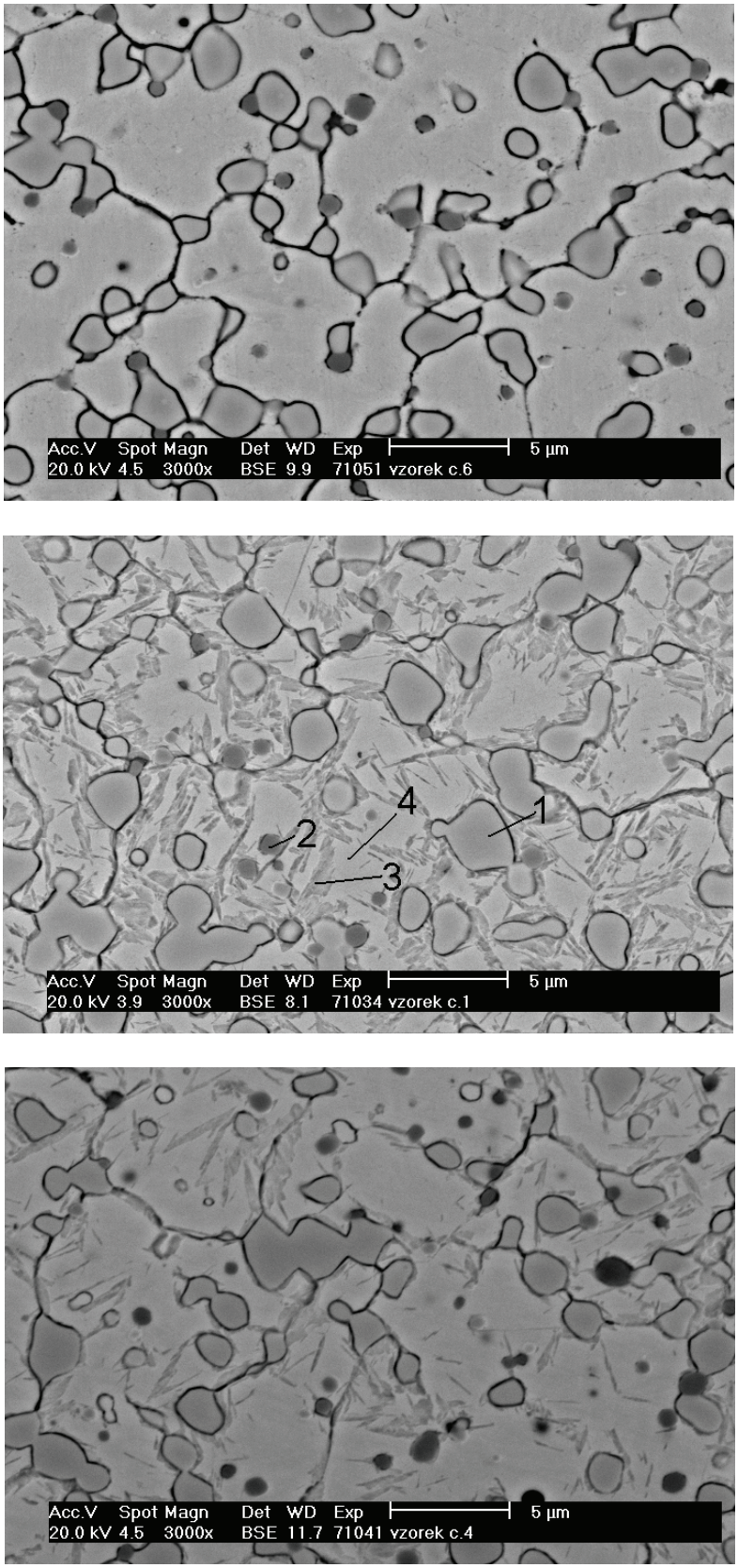


6: *Thermally processed M 390 Böhler steel*
a – Hardened at 1 100 °C for 10 minutes 3 000×
b – Hardened at 1 150 °C for 30 minutes 3 000×
c – Hardened at 1 150 °C for 30 minutes, tempered 3 000×

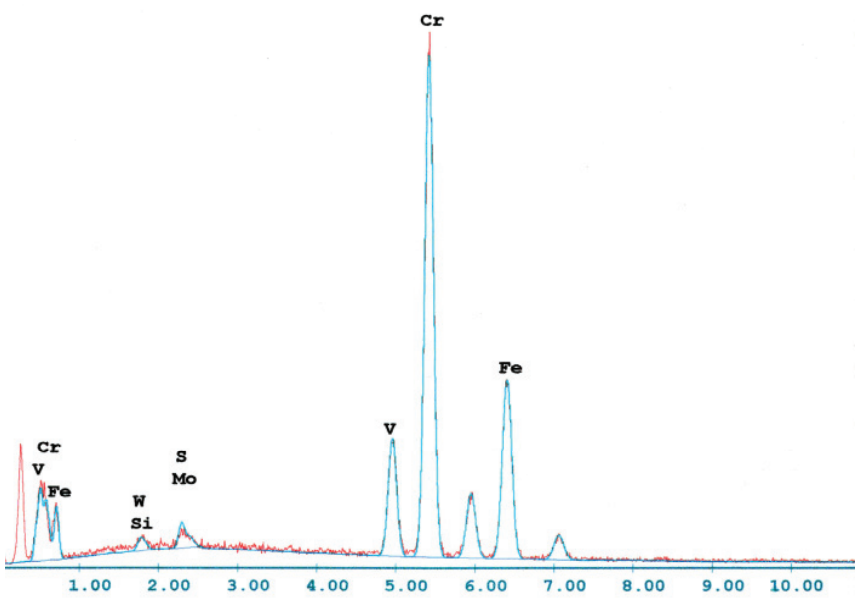


**EDAX ZAF Quantification (Standardless)**
**Element Normalized**
**SEC Table : Default**
**Coating Correction Used : Element : C , Factor : 14.00**

| Element | Wt % | At % | K-Ratio | Z | A | F |
|---|---|---|---|---|---|---|
| SiK | 0.19 | 0.37 | 0.0011 | 1.1257 | 0.4939 | 1.0028 |
| W M | 2.14 | 0.63 | 0.0138 | 0.8542 | 0.7542 | 1.0001 |
| MoL | 2.98 | 1.70 | 0.0229 | 0.9086 | 0.8372 | 1.0067 |
| S K | 0.00 | 0.00 | 0.0000 | 1.1326 | 0.7020 | 1.0076 |
| V K | 10.86 | 11.63 | 0.1080 | 0.9877 | 0.9788 | 1.0289 |
| CrK | 52.13 | 54.70 | 0.5406 | 1.0066 | 0.9883 | 1.0425 |
| FeK | 31.70 | 30.96 | 0.2880 | 1.0089 | 0.8997 | 1.0010 |
| Total | 100.00 | 100.00 | | | | |

**Point 1**

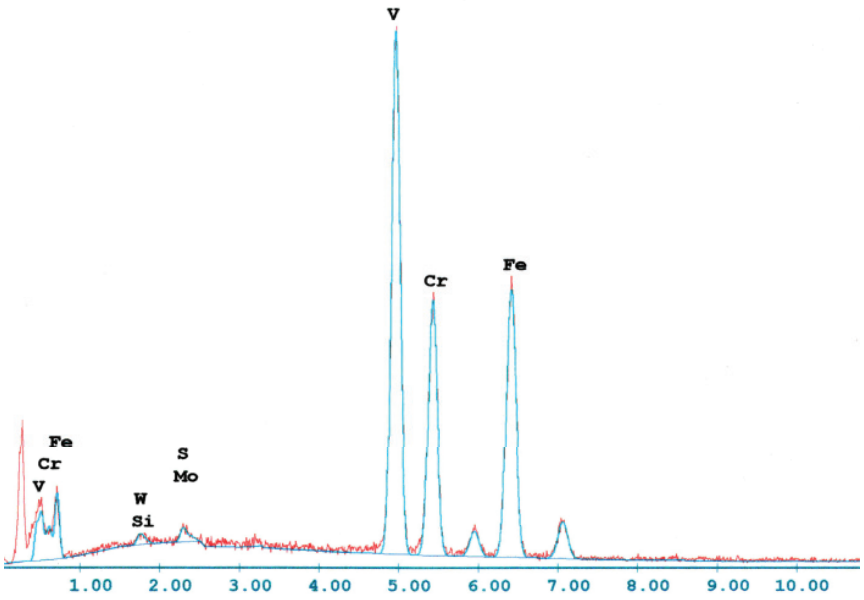


**EDAX ZAF Quantification (Standardless)**
**Element Normalized**
**SEC Table : Default**
**Coating Correction Used : Element : C , Factor : 14.00**

| Element | Wt % | At % | K-Ratio | Z | A | F |
|---|---|---|---|---|---|---|
| SiK | 0.33 | 0.62 | 0.0018 | 1.1288 | 0.4931 | 1.0028 |
| W M | 1.02 | 0.30 | 0.0066 | 0.8566 | 0.7542 | 1.0003 |
| MoL | 1.30 | 0.73 | 0.0101 | 0.9100 | 0.8474 | 1.0074 |
| S K | 0.08 | 0.13 | 0.0006 | 1.1343 | 0.7099 | 1.0086 |
| V K | 40.42 | 42.50 | 0.4101 | 0.9898 | 0.9850 | 1.0406 |
| CrK | 16.84 | 17.35 | 0.1788 | 1.0087 | 0.9932 | 1.0597 |
| FeK | 40.02 | 38.38 | 0.3702 | 1.0107 | 0.9149 | 1.0005 |
| Total | 100.00 | 100.00 | | | | |

**Point 2**

7: *Analysis of the M 390 steel, hardened at 1150 °C for 30 minutes*

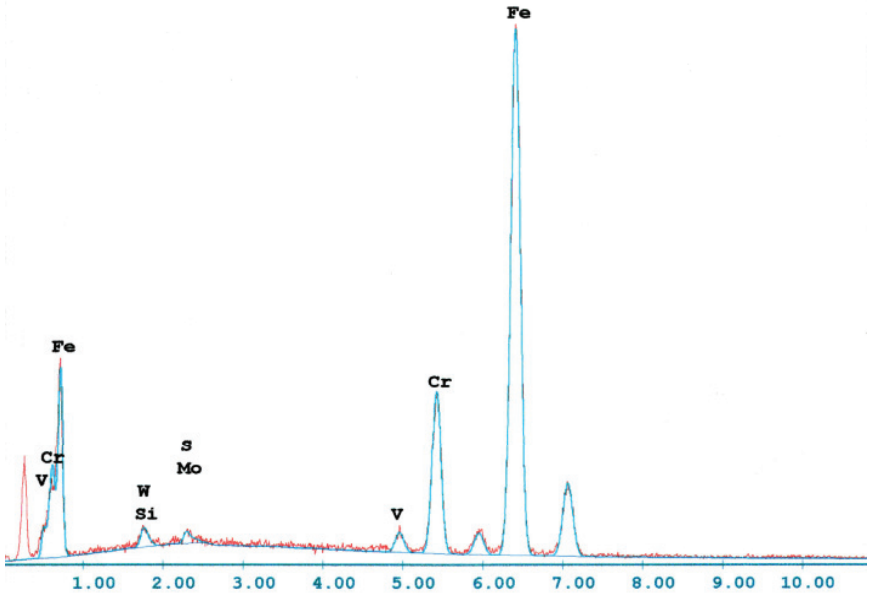


**EDAX ZAF Quantification (Standardless)**
**Element Normalized**
**SEC Table : Default**
**Coating Correction Used : Element : C , Factor : 14.00**

| Element | Wt % | At % | K-Ratio | Z | A | F |
|---|---|---|---|---|---|---|
| SiK | 0.70 | 1.40 | 0.0036 | 1.1191 | 0.4512 | 1.0017 |
| W M | 1.81 | 0.55 | 0.0106 | 0.8492 | 0.6919 | 1.0000 |
| MoL | 1.40 | 0.81 | 0.0100 | 0.9041 | 0.7925 | 1.0015 |
| S K | 0.00 | 0.00 | 0.0000 | 1.1270 | 0.6645 | 1.0049 |
| V K | 1.57 | 1.72 | 0.0168 | 0.9824 | 0.9753 | 1.1188 |
| CrK | 14.07 | 15.11 | 0.1639 | 1.0013 | 0.9856 | 1.1798 |
| FeK | 80.44 | 80.41 | 0.7853 | 1.0037 | 0.9717 | 1.0010 |
| Total | 100.00 | 100.00 | | | | |

**Point 3**

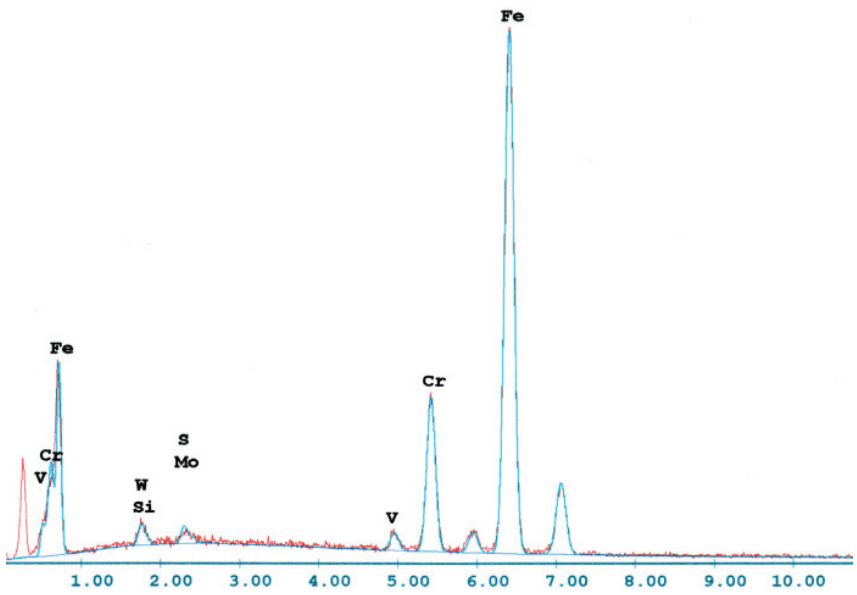


**EDAX ZAF Quantification (Standardless)**
**Element Normalized**
**SEC Table : Default**
**Coating Correction Used : Element : C , Factor : 14.00**

| Element | Wt % | At % | K-Ratio | Z | A | F |
|---|---|---|---|---|---|---|
| SiK | 0.81 | 1.61 | 0.0041 | 1.1196 | 0.4526 | 1.0018 |
| W M | 1.98 | 0.60 | 0.0117 | 0.8496 | 0.6940 | 1.0000 |
| MoL | 2.04 | 1.19 | 0.0147 | 0.9048 | 0.7917 | 1.0015 |
| S K | 0.00 | 0.00 | 0.0000 | 1.1278 | 0.6639 | 1.0049 |
| V K | 1.43 | 1.57 | 0.0153 | 0.9830 | 0.9736 | 1.1177 |
| CrK | 13.60 | 14.65 | 0.1580 | 1.0019 | 0.9842 | 1.1782 |
| FeK | 80.14 | 80.37 | 0.7831 | 1.0044 | 0.9719 | 1.0011 |
| Total | 100.00 | 100.00 | | | | |

**Point 4**

7: *Analysis of the M 390 steel, hardened at 1150 °C for 30 minutes*

is the steel exposed to austentization temperature, the coarser are the carbides. While tempering at secondary hardness, the tempering length affects size and carbide redistribution only. Overall volume fraction of carbides does not change. Their diffuse transformation affects hardness and toughness only as an antecedence of relaxation of inner stress (the second kind). See Fig. 4c.

### The Powdered Steel

Snapshot magnification of 750× to 3 000× was used due to very fine structure of powdered steel. In the supplied state, we can see globular shape of structural phases formed during annealing. Individual snapshots were accompanied with spectral analysis to allow for chemical composition analysis of structural phases.

#### *Basic (Supplied) State*

On the samples (see Fig. 5a) basic surface analysis was performed (due fine grains in the structure, it was only tentative). High zoom reveals primary carbides (see Fig. 5b). Their analysis was performed using a 3000x magnification (see Fig. 5c). Spectral analysis of the snapshots indicates high volume of alloy components in carbides.

#### *Hardened at 1 100 °C for 10 minutes*

Short exposition to quench-hardening temperature is does not trigger spontaneous austenite transformation. Secondary carbides appear the resultant matrix is ferritic (see Fig. 6a). Amount of alloy components from surface analysis data corresponds to amount in the supplied state. However, spectral analysis of carbides shows differences in chemical composition of carbides.

#### *Hardened at 1 150 °C for 30 minutes*

Hardening creates fine pearlite, martensite with a distinct structure, and carbides (fine grain, mostly globular, secondary origin). Residual austenite can be found only in small local areas. Creation of segregation film does not occur due to low volume of sulfur. The snapshot displays typical shapes of chromium carbides, vanadium carbides, and martensite grains (positions 1, 2, 3/4, respectively). Spectral point analysis (see Fig. 7) clearly indicates high volume of chromium (up to 52%) and vanadium (up to 40%) in carbides embedded in the martensitic matrix.

#### *Tempering*

Tempering to secondary hardness refines the appearance of sorbitic structure with globular carbide grains. Stress value decreases after martensitic transformation. This decrease is noticeable in the less distinctive martensite structure. Fig. 6c shows specific shapes of chromium carbides with minimal micro notch effect and shapes of globular vanadium carbides. These are stored in low-energy tempered martensite.

## DISCUSSION

Metallographic analysis can provide solid evidence concerning notch effects of individual structural elements.

The **X2CrNiMo18-14-3** steel (ČSN 17 350) of joint pin is very resistant to corrosion, cannot be hardened, and has a low reactivity with acids (all these properties come from its on industry data sheets). It contains minimal quantity of carbides that are equally dispersed over the whole area. It has high toughness with respect to grains edge shape. These are quite insignificant, which indicates low heterogeneity of the steel composition.

The **X47Cr14** steel (ČSN 17 029) of the scalpel shank shows distinctive structure of acicular martensite (on surface layers). Such structure is not fracture-critical due to tough shank core. In the blade, the carbon is dissolved in individual grains. The steel structure is formed by plate-like martensite with specific grain size (several tens of μm). Carbide distribution is uniform. Grains contain inclusions that had not been completely dissolved during austenitization (induction heating).

The **C80U** steel (ČSN 19 152) in the supplied state has a structure that is defined by granular pearlite with fine carbide distribution. It contains sulfide inclusions that form a distinctive linear pattern. In annealed state, the structure changes into martensite with fine grains containing secondary carbides. In tempered state, the structure is martensitic as well. However, secondary carbides are present in significantly greater amount. Tempering presumably reduces inner stress of the second kind. The structure has very fine grains and therefore exhibits satisfactory fracture behavior. Nucleation and/or critical crack would have to cross tens of grains and large number of edges. The same applies to movement of dislocations in slipping bands that could initiate a microcrack.

The **D2 steel** in annealed state shows the same structure as the C80U steel. Its carbide mesh is finer, clear ferritic grains coexist with clear granular pearlite. When the original pearlite-ferrite structure is hardened at the 1080 °C for 5 minutes and cooled using oil, it changes into ledeburitic structure with secondary carbides. After hardening at 1050 °C for 10 minutes and oil cooling, the structure transforms into eutectic phase with discharged secondary carbides. This means that no standard hardening occurred. Using hardening at 1050 °C for 30 minutes and oil cooling procedure, we get ledeburitic structure again. The longer is the thermal processing, the coarser carbides appear. Tempering decreases inner stress and increases toughness. The ratio of secondary carbides does not change with tempering.

The **M390 Böhler steel** generally shows structure with very fine grains in annealed, hardened and refined states. Grain edges and carbides show very few sharp outlines. High RSP steel toughness probably results from absence of structural micro

notches. Thus, stress concentration caused by notch effect on edges of grains does not occur. According to most commonly accepted fracture mechanics models, very fine grains do not provide condition for possible nucleation of microcracks in martensite packets (see Figure 8). An exception to this concept might be high-speed-loading model. This speed is connected with strain mechanism caused by twin band development. Quoting complete and exact material property information (by manufacturer!) is vital. This includes grain size, size and distribution of carbides, surface energy, γ (this value significantly affects critical fracture stress value), yield stress, and fracture toughness. With this data available, it could be possible to define size of critical crack using shape function of the body produced of the RSP steel and loading type. Size of such crack could be then compared with the observed structure geometry. The verification would definitely confirm data obtained using material analysis.

Carbides contain high volume of bearings (additive metals). See structural analysis data for more information. Hardening from the 1150 °C with short thermal exposition does not perform requested hardening modification. Tempering does not change the volume of alloy components in carbides. The surface analysis confirmed the same amount of bearings (additive metals) as in the non-hardened state.

When the quench-hardening temperature exposure is long, a fine martensitic structure with distinctive martensite and carbide structure is created. Residual austenite is present in minimum amount. Zero sulfur volume prevents creation of segregation film. Point analysis using SEM clearly indicates high volume of chromium (up to 52%) and vanadium (up to 40%) in carbides. Without any doubt, tempering affects value of inner stress after martensitic transformation. This decrease is noticeable as less distinct martensitic structure in all observed samples. The relief does not change even after repeated metallographic preparation with extensive etching times. This indicates change of energetic conditions on martensite packet edges.

The statements listed above are all based on fundamental premise that the basic steel structure is martensite. Later, it is refined using tempering process. Result of this heat treatment under real-life conditions is the presence of other decomposition structures, e.g. bainite or pearlite. Steel resistance against brittle fracture (fatal steel degradation process) could be increased by the following measures:

- Creation of a finer structure (e.g. using thermo-mechanical processing to decrease martensite packet size).
- Increase of refinement and homogeneity of primary steel structures and overall steel purity.

Theoretical prediction concerning increase of polycrystalline material toughness and the results in the paper (metallographic description of RSP steel microstructure) are clearly in compliance (Vlach, 2012).

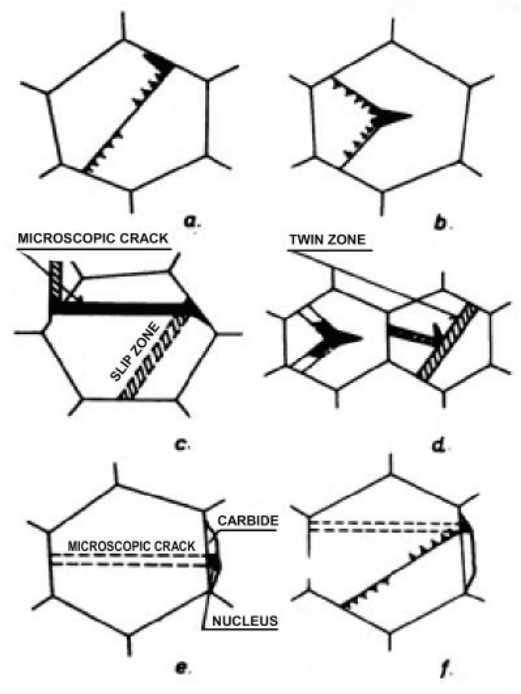


8: *Examples of microcrack nucleation (Vlach, 2012)*

## SUMMARY

Presented paper reviews isochronous metallurgical development of high-grade steels (17 and 19) that are compared with RSP steel (powdered steel).

First part of the paper generally summarizes knowledge about powder metallurgy and application of this progressive technology in steel manufacturing industry. RSP steel advantages are outlined in the fracture mechanics terms with respect to microstructure.

Experimental part deals with structural quality of chosen stainless/tool steel types and allows for comparison of these steel alloys with the M390 Böhler powdered steel.

The comparison was done using a metallographic observation. Steel structures are obviously homogenous, with strict corrosion immunity requirements (grade 17 steels) and wear/strength resistance (grade 19 steels). As far as hardness and toughness are concerned, such standard steels cannot stand against RSP steel (M390). The RSP steel brings on excellent fine grains of martensite and

density of carbides. This structure reduces microstructure notch effect and eliminates segregation film/inclusion development. As a result, directional anisotropy of mechanical properties is minimal. The characteristics listed above deliver outstanding steel resistance. Hardness (up to 65 HRC as reported by manufactures) and toughness (cca 18 $J.cm^{-2}$ by Charpy test, U-notch), represent maximum possible values for steel alloys processing (e.g. forming, thermal processing etc.). Uniform and very fine martensitic packet structure along with fine dispersion of carbides with high volume of vanadium and chromium meet highest construction material requirements in terms of corrosion resistance, hardness properties, and abrasion resistance. Outstanding endurance of these materials means that they can be utilized for special applications, such as splitting tool blades. Observations of characteristic RSP steel structure clearly prove compliance with expert assumptions of theoretical strength. Thus, financial aspect of powdered material manufacturing is the only limitation for extensive application of these state-of-art materials. RSP steel price is often more than ten times the price of conventionally produced steel (e.g. steel for the mold of conventional steel Bohler M 200 is for 70 CZK / kg, by the RSP steel M 390 is for 950 CZK / kg).

Acknowledgement

The present work has been supported by European Regional Development Fund in the framework of the research project NETME Centre under the Operational Programme Research and Development for Innovation (reg. No. CZ. 1.05/2.1.00/01.0002).

## REFERENCES

PTÁČEK, L. a kol., 2002: *Nauka o materiálu II*. 2. vyd. Brno: Akademické nakladatelství CERM, s. r. o., 392 s. ISBN 80-7204-248-3.

KRAUS, V., 2000: *Tepelné zpracování a slinování*. 2. vyd. ZČU Plzeň: 274 s., ISBN 80-7082-582-0.

ČERNÝ, M.: Nožířské oceli – vlastnosti. URL: www.noze-nuz.com (cit. 11. 7. 2012).

HOSFORD, W. F., CADDEL, R. M., 2007: *Metal Forming*. Mechanics and Metalurgy. 3th ed. New York, Cambridge University Press, 365 s., ISBN 978-0-521-88121-0.

FRANTA, J.: Atomizace. URL: http://puskar.webnode.cz/rwl-34/. (cit. 11. 7. 2012).

Nauka o materiálu, Základy lomové mechaniky, URL: http://www.339.vsb.cz/nauka o materialu/Slide5_ZakladyLomoveMechaniky.pdf. VŠB TU Ostrava (cit. 11. 7. 2012)

HALBICH, J., 2009: *Využití korozivzdorných práškových ocelí ve výrobě nástrojů*. Bakalářská práce, MZLU v Brně.

HALBICH, J., 2011: *Výroba nástrojů pseudopráškovou metalurgií*. Diplomová práce, Mendelova univerzita v Brně.

VLACH, B.: Lomové tranzitní chování ocelí, 8 s., wood.mendelu.cz/cz/.../Vlach%20.../05_lomove_chovani_oceli.doc (cit. 11. 7. 2012).

Address

doc. Ing. Michal Černý, CSc., doc. Ing. Josef Filípek, CSc., Mgr. David Varner, Ústav techniky a automobilové dopravy, Mendelova univerzita v Brně, Zemědělská 1, 613 00 Brno, Česká republika, doc. Ing. Pavel Mazal, CSc., Ústav konstruování, Vysoké učení technické v Brně, Technická 2896/2, 616 69 Brno, Česká republika, e-mail: michalc@mendelu.cz, filipek@mendelu.cz, info@davar.cz, mazal@fme.vutbr.cz